A Novel Bounding Surface Constitutive Law for the Monotonic and Cyclic Hardening Response of Metals

Y.F. Dafalias
College of Engineering, Dept. of Civil Engineering,
University of California, Davis, California 95616, U.S.A.

SUMMARY

A particularly simple and efficient constitutive model for the monotonic and cyclic response of hardening metals is presented and analytically formulated for the uniaxial stress space, within the general framework of "Bounding Surface" rate independent elastoplasticity.

The salient feature of plasticity with a bounding surface in stress space is that plastic deformation can occur for stress states within the surface at a rate which depends on the distance δ of the actual stress point from an "image" stress point on the surface, defined by means of an appropriate mapping rule. This is achieved by rendering the actual plastic modulus a function of δ and the bounding plastic modulus associated with the image stress point and obtained by the consistency condition for the bounding surface.

Attention is focused on the uniaxial stress space where the bounding surface degenerates into two points tracing "bounds" in the stress-strain space towards which any stress-strain curve eventually converges. The evolution of these bounds is described by a combination of kinematic and isotropic hardening. The kinematic hardening uses a first back stress associated with the saturated dislocation state reached after extensive plastic loading. A novel feature is the decomposition of the isotropic hardening, measuring dislocation densities, into monotonic and cyclic parts which may interchange and possibly overlap, reflecting the differences and similarities of the dislocation mechanisms under monotonic and cyclic loading.

In the past, the evolution of the actual stress was coupled to that of the "image" stress by using a yield surface always enclosed by the bounding surface and hardening in a coupled way. Here a novel formulation is presented where no yield surface is defined explicitly, and instead a second back stress is introduced, associated with the more "mobile" dislocations before saturation and macroscopically represented by a point moving within the hardening bounding surface. A purely elastic range, called elastic nucleus, is indirectly defined around the second back stress by rendering the plastic modulus infinite when δ satisfies certain conditions of proximity. The evolution of this back stress in the uniaxial space is characterized by a properly changing modulus which is coupled to the actual and bounding plastic moduli introduced earlier. Thus, by means of the evolution of the bounds and the second back stress, a variety of phenomena can be realistically described such as smooth elastoplastic transition, Bauschinger effect, monotonic and increasing strain level cyclic test hardening, lowered yield for reloading after partial unloading, "plateau" response, stabilized and bounded "ratcheting" behavior, etc. One of the attractive features of the model is the small number of the necessary internal variables, which renders its numerical implementation especially tractable for large scale computations.

1. INTRODUCTION

The concept of the "Bounding Surface" in stress space offers a general framework within which the monotonic and cyclic loading response of rate independent elasto-plastic materials can be realistically described. Originally introduced for metals [1-4] and subsequently extended to soils [5,6], the concept can be briefly described as follows. Uniaxial loading shows that any stress-strain curve converges wtih specific and possibly changing "Bounds" in the stress-strain space σ-ε, at a rate which depends on the proximity of the σ-ε point to the bound. Generalizing the concept of the bounds in the multiaxial stress space, a bounding surface is defined on the basis of past loading history which is expressed by means of proper plastic internal variables q_n. The stress point lies within or on the surface, and an appropriate mapping rule associates to the actual stress a unique "image" stress point on the surface, where the normal defines the loading-unloading direction. The plastic modulus is a function of a "bounding" plastic modulus associated with the image stress and obtained by the consistency condition for the bounding surface, and the Euclidian distance δ between actual and "image" stress points. In the course of plastic deformation the value of the plastic modulus changes with δ, and eventually the stress point may contact, but not cross, the surface when $\delta=0$, becoming identical with its image. Upon unloading the stress point detaches from the surface and so forth. During this process the salient feature is that plastic deformation can occur for stress points within the surface at a rate (not time rate) which depends on δ by means of the changing plastic modulus.

In the original formulation [1-3] a classical yield surface was always enclosed by the bounding surface and the mapping rule was obtained by associating actual and image stress points on the yield and bounding surface, respectively, which are characterized by identical directions of the corresponding normals. The smooth elasto-plastic transition was preserved at the expense of an undesirable feature : upon partial unloading-reloading an unrealistic, though small and bounded, "jump" of the stress-strain curve occurred [1,7].

In this paper a novel formulation is presented mainly for the uniaxial stress space, which is void of the above deficiency and which was first conceived in [8]. In addition, it offers greater simplicity by not introducing explicitly a yield surface. The main novel features are the introduction of a "back" stress associated with very mobile dislocations and a decomposition of the isotropic hardening of the bounding surface into interchangeable and possibly overlapping monotonic and cyclic parts.

2. QUALITATIVE DESCRIPTION

The basic qualitative model description is illustrated in Fig. 1 for the multiaxial stress space. The q_n defining the bounding surface $F=0$ are the coordinates β_{ij} of its center, and its size. The β_{ij} represents a rather uniform back stress associated with a saturated state, and the size measures macroscopically the associated dislocation density. A second back stress, the main novel feature, is represented by a point α_{ij} moving within the surface and is associated with the more "mobile" dislocations before saturation. For a stress σ_{ij}, the image stress $\bar{\sigma}_{ij}$ is defined by a simple radial mapping rule [8] as the intersection of $\alpha_{ij}\sigma_{ij}$ with $F=0$. The normal $\underset{\sim}{\nabla}F$ at $\bar{\sigma}_{ij}$ transfers to σ_{ij} defining the loading-unloading direction. This mapping defines indirectly (not explicit description) a loading surface through σ_{ij} [9], which is homeothetic to $F=0$ with α_{ij} the center of homeothecy (but not the center of the loading surface). For any loading rate $\dot{\sigma}_{ij}$, the α_{ij} moves towards σ_{ij} (observe $\dot{\alpha}_{ij}$ in Fig. 1) and the bounding surface hardens isotropically and kinematically. Instrumental during this coupled process are the stress quantities δ and r, eloquently defined in Fig. 1, on which

the plastic modulus depends. A purely elastic range, called "Elastic Nucleus," can be defined around the back stress α_{ij} by simply rendering the plastic modulus infinite when $\delta \geq r/s$, where $s \geq 1$ is the elastic factor. A stress moving from within the elastic nucleus, crosses its boundary at σ^e_{ij} and moves outside with a smooth elasto-plastic transition. Thus, although the boundary of the elastic nucleus is equivalent to the concept of a yield surface, it is not identical since the stress point does not necessarily stay on it, i.e. no consistency condition is required for the elastic nucleus.

In Fig. 2 the uniaxial counterpart is illustrated in the stress-plastic strain space σ-ε^p. The bounds are shown for simplicity by straight lines X'X, Y'Y. For a given ε^p, the actual stress σ, the back stresses α and β, the image stress $\bar{\sigma}_+$ (or $\bar{\sigma}_-$ if σ lies below α) and the smooth elasto-plastic transition points σ^e_+ and σ^e_- defining the range of elastic nucleus, are shown on a vertical line with the same abscissa ε^p. The distances $\delta = |\bar{\sigma}_+ - \sigma|$ and $r = |\bar{\sigma}_+ - \alpha|$ are also shown. For any rate $\dot{\varepsilon}^p$ the $\bar{\sigma}_+$, σ, α and β move along specific curves according to moduli $\bar{E}^p$ (bounding plastic modulus), E^p (actual plastic modulus), E^p_α and E^p_β, respectively. If E^p_o represents the constant limiting value of $\bar{E}^p$, it will be taken here $E^p_\beta = E^p_o$. For straight line bounds also $\bar{E}^p = E^p_o$. The interrelation among these moduli, which is achieved by means of δ, r, s and proper material constants, is the key to the analytical formulation. Observe that upon partial unloading at σ at a level between σ and σ^e_+ (defined by $\delta = r/s$) and subsequent reloading, a lower yield point is obtained immediately upon reloading and the curve converges at c with the previous one (if unloading has not occurred). For unloading below σ^e_+ and reloading, yield initiates at σ^e_+ with smooth elastoplastic transition. For purely linear kinematic hardening the bounds are straight lines, as shown in Fig. 2, but this is not true if isotropic hardening causes the size k to change (2k=distance between bounds).

3. ANALYTICAL DESCRIPTION IN UNIAXIAL STRESS SPACE

Based on the above qualitative description, the uniaxial analytical formulation is obtained as follows. The bounding surface is defined by

$$F = (\bar{\sigma} - \beta)^2 - k^2 = 0 \tag{1}$$

Loading occurs whenever $(\bar{\sigma}-\beta)\dot{\sigma} > 0$ and this is implied henceforth. For a plastic strain rate $\dot{\varepsilon}^p$, the stress quantities obey:

$$\dot{\varepsilon}^p = \frac{\dot{\sigma}}{E^p} = \frac{\dot{\bar{\sigma}}}{\bar{E}^p} = \frac{\dot{\alpha}}{E^p_\alpha} = \frac{\dot{\beta}}{E^p_o} \tag{2}$$

The $\bar{E}^p$ will be obtained from the consistency condition $\dot{F}=0$, E^p_o is a material constant associated with saturated states, and the following relations are proposed for E^p, E^p_α in terms of r and δ:

$$E^p = \bar{E}^p + \frac{Eh\delta}{\langle r - s\delta \rangle} \tag{3}$$

$$E^p_\alpha = \bar{E}^p + \left(\frac{r}{2k} - \frac{1}{m}\right) \frac{Ezr}{\langle r - s\delta \rangle} \tag{4}$$

where E is the elastic modulus for non-dimensionalization, h, z, m are material constants and the brackets define the operation $\langle x \rangle = xH(x)$ with H being the heavyside step function. Essentially eqs. (3) and (4) are the differential equations of the σ-ε^p and α-ε^p curves. Observe that for $\delta \geq r/s$, eqs. (3) and (4) yield $E^p = E^p_\alpha = \infty$ (elastic nucleus and smooth elasto-plastic transition). As $\delta \to 0 \Rightarrow E^p \to \bar{E}^p$ which implies that the stress converges with the bound. As $r \to (2k/m) \Rightarrow E^p_\alpha \to \bar{E}^p$, which implies that α converges

with a curve parallel to the bound at a distance 2k/m. For $m=\infty$ and $r\to 0$ (this implies $\delta\to 0$ since $r>\delta$), α also converges with the bound. The most important parameters are s, h and z, and m can usually be taken in the range of 20-50. In order to obtain a continuously decreasing E^p, the condition $dE^p<0$ must be imposed. For constant $\bar{E}^p=E_o^p$ and s, this implies $d(r/\delta)>0$ which on the basis of eqs. (2), (3) and (4) yields the following restriction on the material constants:

$$z < \frac{m}{m-2}\, h \tag{5}$$

obtained in the limit by requiring $dE^p<0$ at $E^p=\infty$ as $r\to s\delta$.

Attention now will be focused on the evolution of the bounds or $\bar{\sigma}$, i.e. the hardening of the bounding surface for the determination of $\bar{E}^p$. The kinematic hardening is fixed by taking $\dot{\beta}=E_o^p\dot{\varepsilon}^p$ (more general rules can be introduced if necessary). To account for a slight asymmetry of the stress-strain curve between tension and compression, an initial small value $\hat{\beta}$ (usually negative) can be assigned for β at $\varepsilon^p=0$. It is only the isotropic hardening, expressed by the change of k, which needs special attention.

The value of k is a macroscopic measure of the dislocation density which changes in a different way under monotonic and cyclic loading. This, of course, brings the question of the exact definition of what is monotonic and what is cyclic loading. To this extent, one may introduce the following quantities:

$$\lambda_{max} = \Delta\varepsilon^p_{max} = \varepsilon^p_{max} - \varepsilon^p_{min} \tag{6a}$$

$$\lambda_o = (\varepsilon^p_{max} + \varepsilon^p_{min})/2 \tag{6b}$$

$$\lambda = 2(\varepsilon^p - \lambda_o) \tag{6c}$$

$$\ell = \dot{\varepsilon}^p\lambda = 2\dot{\varepsilon}^p(\varepsilon^p-\lambda_o) \tag{6d}$$

where λ_{max} represents the maximum plastic strain range the material has experienced in its past loading history, λ_o is the center of this range, $\lambda/2$ measures the plastic strain "distance" of the current ε^p from λ_o, and ℓ is a plastic strain rate loading function. Pure monotonic loading, associated with dislocation glide in one direction, is defined as the process of increasing λ_{max}, i.e. when $|\lambda|=\lambda_{max}$ and $\ell>0$. This implies that $\varepsilon^p=\varepsilon^p{}_{max}$ or $\varepsilon^p=\varepsilon^p{}_{min}$ and $\dot{\varepsilon}^p$ is directed outwards from the domain defined by λ_{max}. The $|\lambda|<\lambda_{max}$ defines a state under a predominantly cyclic loading condition, being associated with cyclic glide processes. It is still possible however, that even with $|\lambda|<\lambda_{max}$ a small amount of monotonic hardening may simultaneously occur when $\ell>0$, depending on $|\lambda|/\lambda_{max}$, which leaves however λ_{max} fixed until $|\lambda|=\lambda_{max}$. As $|\lambda|/\lambda_{max}\to 1$ a smooth interchange from a predominantly cyclic to a pure monotonic hardening occurs.

Reflecting the differences of monotonic and cyclic isotropic hardening, the rate $\dot{k}$ can be decomposed into a monotonic $\dot{k}_m$ and a cyclic $\dot{k}_c$ part, each being linearly dependent on the cumulative plastic strain rate $\dot{\bar{\varepsilon}}^p=|\dot{\varepsilon}^p|$, i.e.:

$$\dot{k} = \dot{k}_m + \dot{k}_c = (W_m + W_c)\,\dot{\bar{\varepsilon}}^p \tag{7}$$

where the smooth interchange and possible slight overlapping between monotonic and cyclic hardening discussed above can be analytically described by setting:

$$W_m = w\, C_m(k_{sm} - k_m) \tag{8a}$$

$$W_c = (1 - w)\, C_c\, (k_{sc}\,(\lambda_{max}) - k_c) \tag{8b}$$

$$w = H(\ell)\ (|\lambda|/\lambda_{max})^n \tag{8c}$$

with k_{sm} being the saturated value of k_m, k_{sc} the saturated value of k_c which depends on λ_{max}, C_m and C_c are material constants associated with the rapidity of saturation, H is the heavyside function and n a material constant which assumes usually large values of the order of 50 or more. Observe from eqs. (7) and (8) that when $(|\lambda|/\lambda_{max})=1$ and $\ell>0 \Rightarrow w=1$ (pure monotonic hardening), while when $|\lambda|/\lambda_{max}<1$, w=0 if $\ell<0$ (only cyclic hardening) or $w<<1$ if $\ell>0$ due to the large value of n (predominantly cyclic hardening with some small monotonic contribution). As $n\to\infty$ no monotonic occurs for $|\lambda|<\lambda_{max}$ irrespective of the sign of ℓ.

Based on eqs. (1), (7), (8) and $\dot{\hat{\beta}}=E_o^p\dot{\varepsilon}^p$, one has from the consistency condition $\dot{F}=0$:

$$\bar{E}^p = E_o^p + W_m + W_c \tag{9}$$

Observe that when saturation occurs $k_m\to k_{sm}$ and $k_c\to k_{sc}$, thus W_m, $W_c\to 0$ which yields $\bar{E}^p=E_o^p$, i.e. only kinematic hardening occurs and the bounds assume a constant slope E_o^p. For materials without significantly different hardening response between cyclic and monotonic loading, one can redefine w=1, thus $W_c=0$ and $W=C_m(k_{sm}-k_m)$. A nice multiaxial generalization of the concept of λ_{max} and λ_o was given in [10] by means of a plastic strain memory hypersphere as well as the concept of loading-unloading for states on the hypersphere, i.e. $|\lambda|=\lambda_{max}$. The loading-unloading condition as defined by eq. (6d) for $|\lambda|<\lambda_{max}$ appears to be novel, and essentially introduces a bounding hypersphere in the plastic strain space rather than a loading one as suggested in [10].

To complete the set of necessary equations one has only to define the dependence of k_{sc} on λ_{max}. This can be easily obtained from

$$k_{sc} = \sigma_c\left(\frac{\lambda_{max}}{2}\right) - \left[E_o^p\,\frac{\lambda_{max}}{2} + \hat{\beta}\right] - k_m \tag{10}$$

where σ_c is the cyclic stress, i.e. the locus of the tips of the stabilized cyclic loops in an increasing strain level cyclic tests, and the subtraction of the last two terms aims at excluding the contribution of kinematic and monotonic isotropic hardening to the value of σ_c. For constant λ_{max} it is possible to have a slight change of k_{sc} as k_m may undergo a small change even under cyclic loading (recall eqs. (8)). A very simple curve fitting of σ_c can be achieved by a three parameters equation of the form:

$$\sigma_c = d_1 + d_2\left(\frac{\lambda_{max}}{2}\right)^{d_3} \tag{11}$$

4. DETERMINATION OF MATERIAL CONSTANTS

4.1 Constants associated with the image stress and the bounds

The E_o^p is determined from the final slope E_o^t of the monotonic curve in the σ-ε space and E, by means of $E_o^p=EE_o^t/(E-E_o^t)$. The k_{sm} is obtained from the monotonic curve by $k_{sm}=\sigma-E_o^p\varepsilon^p$ after convergence with the bound. The k_{sc} is not a material constant, but is determined from eqs. (10) and (11) by means of three constants d_1, d_2, d_3. The constants C_m, C_c are determined from monotonic and cyclic curves converged with the bounds, after eqs. (7) and (8) are integrated yielding:

$$C_i = \frac{1}{\bar{\varepsilon}^p - \bar{\varepsilon}^p_o} \ell n \left(\frac{k_{si} - k_{oi}}{k_{si} - k_i} \right) \qquad (12)$$

where i stands for either m or c, and k_{oi}, $\bar{\varepsilon}^p_o$ are initial values. Finally $\hat{\beta}$ is determined from the slight asymmetry of the bounds and n is usually chosen very large, i.e. n≃100.

4.2 Constants associated with the actual stress and mobile back stress

These are the s, h, z and m. The s can be determined as the ratio of the elastic nucleus size to that of the bounding surface, which can be obtained by locating after partial unloading the subsequent yield points in reloading and reversed loading. The m varies usually between 20-50, and can be determined by partial unloading-reloading after extensive monotonic loading which ensures converges with the bound. The h, z are determined from stabilized loops as follows. One can substitute δ and r in terms of $\bar{\sigma}$, σ and α in eqs. (3) and (4). Then, recalling that $d\sigma/d\varepsilon^p = E^p$ and $d\bar{\sigma}/d\varepsilon^p = E^p_o$, one can eliminate α and $d\alpha/d\varepsilon^p$ from eqs. (3) and (4) to obtain a second order differential equation for σ in terms of h and z. Since it is not possible to solve it due to high nonlinearity, one may curve-fit the experimental curve by another simple equation and then substitute the derivatives of this equation into the above differential equation, thus obtaining numerically the h, z from two points on the experimental curve. Closed form expressions have been developed for h, z, which must satisfy the condition (5).

Two sets of constants are shown in Table 1. Their total number is 14, but since n is fixed at 100 their actual number is 13. If no distinction between cyclic and monotonic isotropic hardening is made, their number is reduced to 9 (set 1).

5. COMPARISON WITH EXPERIMENTS

Before the actual comparison, Fig. 3 shows eloquently some of the basic features of the model, using the set 1 of material constants. Smooth elasto-plastic transition and lower yield at reloading after partial unloading are described, and stabilized "ratcheting" response is easily obtained as the mobile back stress α moves upwards and brings the oscillating stress completely within the elastic nucleus. The "plateaux" on the α curves indicate $\dot{\alpha}=0$ while the strain changes elastically.

Fig. 4 shows comparison between the present constitutive model and experimental curves for A106 steel ($E=2.45\times10^4$KSI, slightly smaller than for initial elastic loading) obtained in [11], as well as the curves traced by the mobile back stress α. The set 1 of material constant was used after calibration for the curves. Only monotonic isotropic hardening was considered (9 parameters). The plateau needed special treatment, keeping the slope of the bound equal to zero and using high values of h, z for the plateau range (about 30 times the normal values). The agreement is seen to be very good, with the prediction being sometimes almost indistinguishable from the experiment.

Figures 5b,c show the model predictions associated with the experimental curves, Figs. 5a,b, on 316L stainless steel ($E=1.51\times10^5$ MPa) as reported in [10]. The set 2, Table 1, of material constants was used after calibration on the basis of the outer loops in Fig. 5a and the monotonic and cyclic curves in Fig. 5b. No isotropic hardening was assumed for the monotonic loading (observe $C_m=0$ and $k_{sm}=k_{om}$: constant), i.e. the monotonic bound is a straight line, Fig. 5b. The agreement between theory and experiment for both monotonic loading, and increasing strain level cyclic loading is seen to be very good. Especially the final slopes of the stabilized loops being equal to E^p_o (computed from the E^t_o shown in Fig. 5b) are in very good agreement with the experiments, a point where the corresponding model presented in [10] was not entirely successful for the smaller strain

amplitudes, and which may cause great deviation if monotonic loading continued towards larger strains after stabilization. The back stress α versus ϵ is shown finally in Fig. 5d.

ACKNOWLEDGEMENT

The author wishes to acknowledge the contribution of Mr. S.M. Seyed-Ranjbari, graduate student in the Department of Civil Engineering of U.C. Davis, who implemented the model numerically and assisted in the calibration of the material constants.

Table 1. Two Sets of Material Constants

Constant	Set 1	Set 2	Constant	Set 1	Set 2
E_o^p	305 KSI	1.46×10^3 MPa	k_{sm}	60.5 KSI	340 MPa
s	2.18	2.10	k_{om}	47.4 KSI	340 MPa
h	0.23	0.26	d_1	—	170 MPa
z	0.25	0.28	d_2	—	2411 MPa
m	23	21	d_3	—	0.453
C_m	36	0	$\hat{\beta}$	-1.22 KSI	-14 MPa
C_c	—	8	n	—	100

REFERENCES

[1] DAFALIAS, Y.F., "On Cyclic and Anisotropic Plasticity," Ph.D. Dissertation, Department of Civil Engineering, U.C. Berkeley (1975).

[2] DAFALIAS, Y.F., POPOV, E.P., "A Model of Nonlinearly Hardening Materials for Complex Loading," **Acta Mechanica,** Vol. 21, No. 3, pp. 173-192 (1975). Proceedings of the 7th U.S. National Congress of Applied Mechanics, p. 149, Boulder, Colorado, 1979.

[3] DAFALIAS, Y.F., POPOV, E.P., "Plastic Internal Variables Formalism of Cyclic Plasticity," **J. Appl. Mech.,** Vol. 98, No. 4, pp. 645-651 (1976).

[4] KRIEG, R.D., "A Practical Two Surface Plasticity Theory," **J. Appl. Mech.,** Vol. 47, No. E3, pp. 641-646 (1975).

[5] DAFALIAS, Y.F., HERRMANN, L.R., "A Bounding Surface Soil Plasticity Model," **Int. Symp. on Soils under Cyclic and Transient Loading,** Vol. 1, pp. 335-345, Swansea, U.K., 1980.

[6] MROZ, Z., NORRIS, V.A., ZIENKIEWICZ, O.C., "Application of an Anisotropic Hardening Model on the Analysis of Elasto-plastic Deformation of Soils," **Geotechnique,** Vol. 29, No. 1, pp. 1-34 (1979).

[7] PETERSSON, H., POPOV, E.P., "Constitutive Relations for Generalized Loadings," **J. Eng. Mech. Division,** EM4, pp. 611-627, August (1977).

[8] DAFALIAS, Y.F., "The Concept and Application of the Bounding Surface in Plasticity Theory," **Symp. IUTAM, on Physical Non-Linearities in Structural Analysis,** Senlis, France, May 1980, in press.

[9] PHILLIPS, A., SIERAKOWSKI, R.L., "On the Concept of the Yield Surface," **Acta Mechanica,** Vol. I, No. 1, pp. 29-35 (1965).

[10] CHABOCHE, J.L., DANG VAN, K., CORDIER, G., "Modelization of the Strain Memory Effect on the Cyclic Hardening of 316 Stainless Steel," **Trans. of SMiRT 5,** L 11/3, Berlin, August 1979.

[11] POPOV, E.P., PETERSSON, H., "Cyclic Metal Plasticity: Experiments and Theory," **J. Eng. Mech. Division,** EM6, pp. 1371-1388, December (1978).

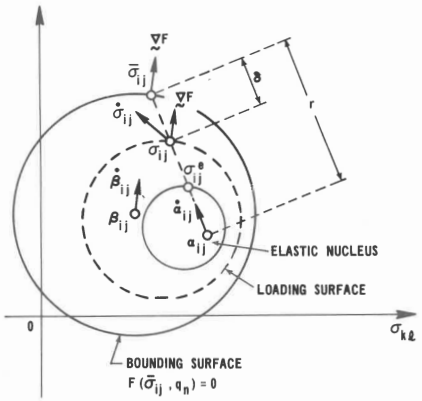

Fig. 1. Schematic illustration of the model in multiaxial stress space

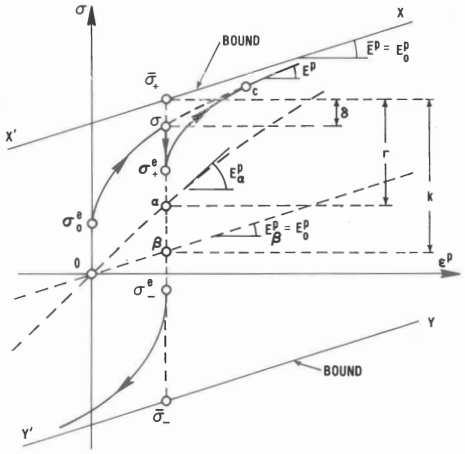

Fig. 2. Schematic illustration of the model in uniaxial stress space

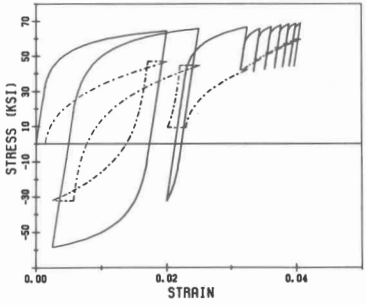

Fig. 3. Qualitative description of the response under random cyclic loading (——), showing also the trace of the mobile back stress α (—•—) and the ratcheting response.

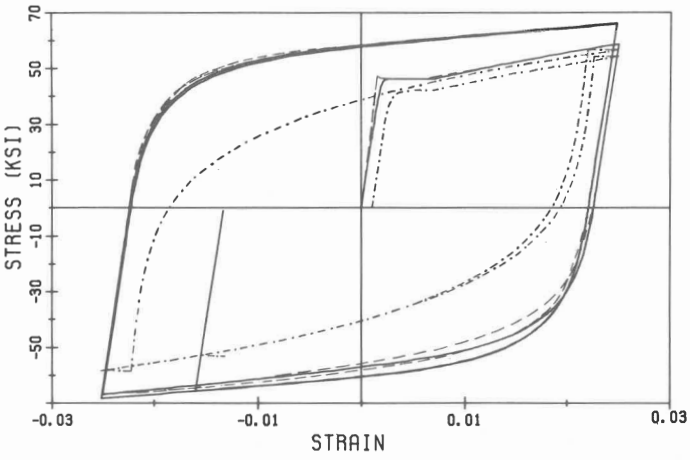

Fig. 4. Theory (——) versus experiment (— —) and the trace of the back stress α (—•—) for cyclic loading of A106 seamless steel pipe. Experimental data after [11].

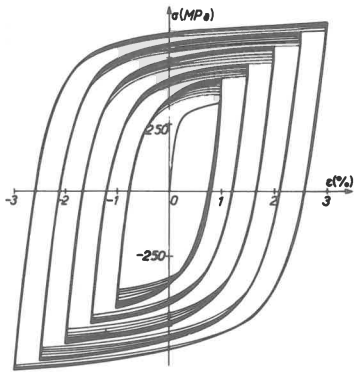

Fig. 5a. Experimental data for increasing strain level cyclic loading of 316L steel, after [10].

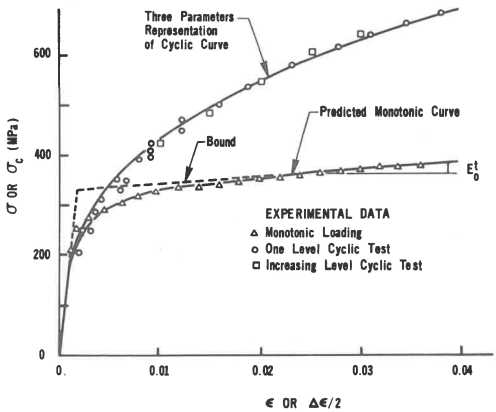

Fig. 5b. Monotonic and cyclic stress-strain curves for 316L steel and their modelization. Experimental data after [10].

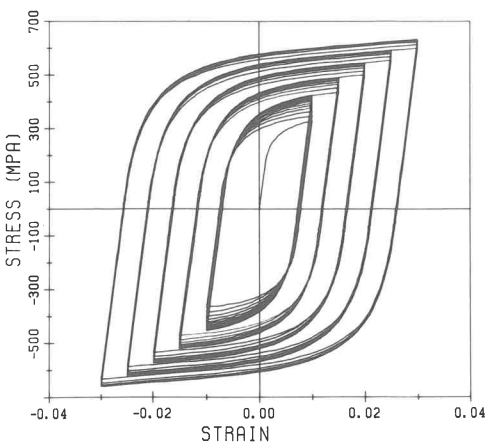

Fig. 5c. Model prediction of the experimental stress-strain curves shown in Fig. 5a.

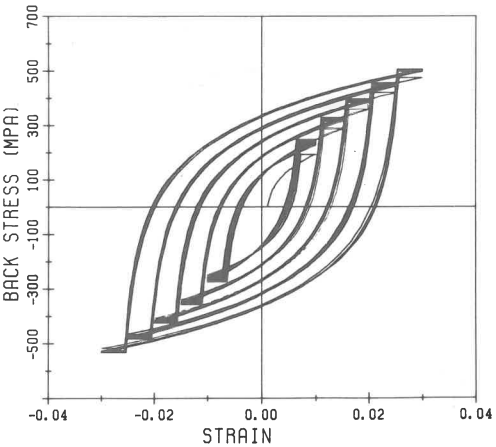

Fig. 5d. The trace of the back stress α for the cyclic loading response shown in Fig. 5c.